AIAA 80-1021R

Noise Caused by the Interaction of a Rotor with Anisotropic Turbulence

E. J. Kerschen*
General Electric Corporate Research and Development, Schenectady, N.Y.
and
P. R. Gliebe†
General Electric Aircraft Engine Business Group, Evendale, Ohio

An analytical model of fan noise caused by inflow turbulence, a generalization of earlier work by Mani, is presented. Axisymmetric turbulence theory is used to develop a statistical representation of the inflow turbulence valid for a wide range of turbulence properties. Both the dipole source due to rotor blade unsteady forces and the quadrupole source resulting from the interaction of the turbulence with the rotor potential field are considered. The effects of variations in turbulence properties and fan operating conditions are evaluated. For turbulence axial integral length scales much larger than the blade spacing, the spectrum is shown to consist of sharp peaks at the blade passing frequency and its harmonics, with negligible broadband content. The analysis can then be simplified considerably and the total sound power contained within each spectrum peak becomes independent of axial length scale, while the width of the peak is inversely proportional to this parameter. Large axial length scales are characteristic of static fan test facilities, where the transverse contraction of the inlet flow produces highly anisotropic turbulence. In this situation, the rotor/turbulence interaction noise is caused mainly by the transverse component of turbulent velocity.

I. Introduction

NOISE caused by ingested turbulence is now recognized as a major source of the differences between aircraft engine noise measurements in test stand facilities and in flight. In static engine tests, this mechanism can cause prominent tones at the blade passing frequency and its harmonics, while it contributes relatively little to the noise measured in flight. Because of their greater flexibility and lower operating costs, it is desirable to use ground-based test facilities for acoustic evaluation of turbofan engines. However, it is important for these static engine tests to reasonably simulate flight noise levels. To examine this issue, the present paper and Ref. 1 present an analytical study of the noise generated by rotor/turbulence interaction. The basic analytical model is developed in this paper. Reference 1 applies this model to a variety of ground-based test facilities and presents a comparison with expected flight noise levels.

The earliest analytical studies of noise generation due to the interaction of turbulence with a rotor were presented by Morfey,[2] Mani,[3] and Homicz and George.[4] These analyses used a statistical representation of the incident turbulence, which was assumed to be isotropic. Subsequent measurements by Hanson[5] showed that, in the static test case, the turbulence impinging on the fan is highly anisotropic with axial integral length scales several hundred times as large as the transverse length scale. This great disparity in length scales is caused by the lateral contraction of the flow as it enters the inlet.

The first analysis which considered the anisotropic nature of the turbulence was presented by Hanson.[5] His model was based on the technique of random pulse modulation. Thus the turbulence was assumed to consist of discrete eddies whose intensity, width, and length were random variables. Utilizing this approach, he derived the far-field noise spectrum for the case of an unducted rotor. The predicted spectrum contained peaks at the blade passing frequency and its harmonics, superposed on a broadband spectrum.

A statistical approach similar to that in Refs. 2-4 can also be used to predict noise generation by anisotropic turbulence impinging on a rotor. To do this, an appropriate model of the anisotropic turbulence must be developed. Pickett[6] modified the analysis of Ref. 3 by assuming an anisotropic correlation function for the velocity component normal to the blade surfaces. Pickett's results clearly show the influence of anisotropy on the noise generation. However, the velocity correlation used in his analysis is not normally measured in experiments and is not independent of fan geometry and operating conditions. Also, Pickett's analysis only included the dipole source term, i.e., the effect of the rotor steady loading was not considered. Chandrashekara[7,8] used a statistical approach to calculate noise generation by an unducted rotor, but only included the axial component of the turbulent velocity field in his model. The results of the present study indicate that, in the static test case ($\ell_a/\ell_t \gg 1$), the transverse component of turbulent velocity is responsible for most of the noise generation. In more recent work, Mani[9,10] modified his model to include the quadrupole source term associated with the rotor steady loading and produced anisotropic turbulence by applying a sudden contraction[11] to the isotropic turbulence spectrum.

In an early phase of the present research program, we examined the application of a sudden contraction to isotropic turbulence as a model for inflow turbulence. Unfortunately, the rapid distortion theory[11] produced length scale and velocity ratios having approximately the same order of magnitude, while the experimental measurements showed that $\ell_a/\ell_t \gg u_t/u_a$. In this paper, we apply the theory of axisymmetric turbulence[12] to develop a turbulence spectrum model that is consistent with the experimental measurements. The model is used to predict the characteristics of fan noise caused by inflow turbulence. Comparisons with experimental data are presented, and a simplified analysis for the case of large axial length scale turbulence is developed.

Presented as Paper 80-1021 at the AIAA 6th Aeroacoustics Conference, Hartford, Conn., June 4-6, 1980; submitted July 21, 1980; revision received Jan. 5, 1981.

*Mechanical Engineer.
†Manager, Aeroacoustic Analysis. Member AIAA.

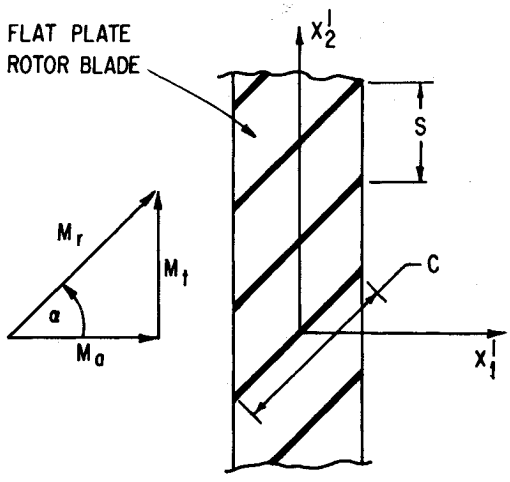

Fig. 1 Fan geometry and coordinate system.

II. Review of Rotor/Turbulence Interaction Noise Theory

The acoustic analysis used in the present work has been discussed in Refs. 3, 9, and 10 and will be reviewed only briefly here. A two-dimensional representation of the rotor is used, as shown in Fig. 1. Thus, the blades appear as a cascade of flat plates staggered at an angle $\alpha = \tan^{-1}(M_t/M_a)$ to the axial (x_1') direction. The coordinates (x_1', x_2', x_3') are taken as fixed with respect to the casing of the machine. The parameter s is the blade spacing in the x_2' direction. The flow through the rotor consists of a turbulent velocity field convected by a uniform axial mean flow. In addition to this, we have the potential flowfield associated with the rotor steady loading. The turbulent velocity field is represented as a stochastic Fourier-Stieltjes integral of the type

$$v_i = \iiint e^{j\boldsymbol{k}\cdot\boldsymbol{r}} \mathrm{d}Z_i(\boldsymbol{k}) \tag{1}$$

where $\boldsymbol{k}$ is the wavenumber vector and $\boldsymbol{r}$ is the position vector in a frame of reference moving with the uniform mean flow. The $\mathrm{d}Z_i$ obey the statistical orthogonality condition

$$\overline{\mathrm{d}Z_i(\boldsymbol{k})\mathrm{d}Z_j(\boldsymbol{k}')} = \delta(\boldsymbol{k}-\boldsymbol{k}')\Phi_{ij}(\boldsymbol{k})\mathrm{d}\boldsymbol{k}\mathrm{d}\boldsymbol{k}' \tag{2}$$

where Φ_{ij} is the energy spectrum tensor of the turbulence and the overbar denotes an ensemble average.

Two noise source mechanisms are considered. First, we have the dipole noise source associated with unsteady pressures on the blade surfaces. Second, there is a quadrupole source due to the interaction of the turbulence with the rotor potential flowfield. These source mechanisms are analyzed separately and the results combined in a mean square fashion.

To determine the dipole source term, we must calculate the unsteady pressures on the blade surfaces due to the convected turbulent velocity field. This involves the solution of unsteady, three-dimensional, compressible flow through a cascade. Since closed-form solutions are not available for this general case, some assumptions must be made. The model developed in Refs. 3, 9, and 10 assumes that the boundary condition on each blade can be satisfied independently, that a two-dimensional lift response theory is adequate, and that the rotor blades are compact acoustic sources. The final expression for the power density spectrum $P^{\pm}(f)$ radiated upstream and downstream of the rotor is

$$P_d^{\pm}(f/f_b) = \sum_{n=-\infty}^{\infty} \int \tilde{\Phi}_d(k_1,k_2) E_d^{\pm}(k_1,k_2) L^2(\omega)\mathrm{d}k_2 \tag{3a}$$

where we set

$$k_1 = \frac{2\pi}{s}\left(n - \frac{f}{f_b}\right)\tan\alpha \tag{3b}$$

$$\omega = (c/2)(k_1\cos\alpha + k_2\sin\alpha) \tag{3c}$$

and the integration is over the range

$$\frac{2\pi}{s}\left(-\frac{f}{f_b}\frac{M_t}{\sqrt{1-M_a^2}} - n\right) \le k_2 \le \frac{2\pi}{s}\left(\frac{f}{f_b}\frac{M_t}{\sqrt{1-M_a^2}} - n\right) \tag{3d}$$

Here f_b is blade passing frequency and $\tilde{\Phi}_d$ is the two-dimensional spectrum of the velocity normal to the blade chord

$$\tilde{\Phi}_d(k_1,k_2) = \tilde{\Phi}_{11}\sin^2\alpha - 2\tilde{\Phi}_{12}\sin\alpha\cos\alpha + \tilde{\Phi}_{22}\cos^2\alpha \tag{4}$$

$E_d^{\pm}$ are the upstream and downstream acoustic radiation efficiency factors, which are functions of the mean flow and geometry parameters as well as k_1 and k_2. L is the magnitude of the airfoil lift coefficient, which is calculated using Refs. 13 and 14 for low and high reduced frequencies, $M_r\omega/(1-M_r^2) \lessgtr 1$, respectively. For values of k_2 outside the range of the integral, the acoustic waves are cut off and thus do not propagate acoustic energy. For more details on the dipole noise source mechanism, consult Ref. 3.

We will now discuss the quadrupole source term. The analysis for this case is based on a Lighthill type equation modified to account for the uniform mean flow. The source term in the equation is of the form $\partial^2(\rho_0 w_i w_j)/\partial x_i \partial x_j$ where the w_i are the fluctuating velocities associated with the convected turbulence or the rotor potential field. We consider only subsonic rotor speeds and assume that the turbulent velocity fluctuations are very small compared to those of the rotor potential field. Then the only terms that produce appreciable acoustic energy are those representing the interaction between the turbulence and the rotor potential field. The Lighthill type equation is solved as an inhomogeneous equation in the cascade plane without regard to the boundary conditions created by the presence of the rotor blades. The final result for the power spectral density of the noise field can be written in the form

$$P_q^{\pm}\left(\frac{f}{f_b}\right) = \sum_{n=-\infty}^{\infty} \int \tilde{\Phi}_q(k_1,k_2) E_q^{\pm}(k_1,k_2)\mathrm{d}k_2 \tag{5}$$

where again we use Eq. (3b) to replace k_1 and the limits of integration are given by Eq. (3d). The quadrupole spectrum function $\tilde{\Phi}_q$ has the form

$$\tilde{\Phi}_q(k_1,k_2) = \mathcal{G}_1^2\tilde{\Phi}_{11} + 2\mathcal{G}_1\mathcal{G}_2\tilde{\Phi}_{12} + \mathcal{G}_2^2\tilde{\Phi}_{22} \tag{6}$$

Here $\mathcal{G}_i$, $i=1, 2$, are functions of k_1, k_2 and the mean flow parameters and have a linear dependence on rotor lift coefficient C_ℓ. $E_q^{\pm}$ are the upstream and downstream quadrupole acoustic radiation efficiency factors. For more details on the quadrupole source terms, consult Ref. 9.

It can be seen from the preceding summary that the calculation of the noise level at a particular frequency in general involves the summation of an infinite series each term of which includes an integral. In the present work, these integrals were evaluated numerically and the summations were truncated at a finite number of terms. Calculation of the total power output then involves a further integration over frequency. However, for the limit of large axial length scale $(\ell_a/s \gg 1)$, the analysis simplifies considerably, as will be shown in Sec. IV. The limit of large axial length scale occurs often in practical applications.

III. Development of Anisotropic Turbulence Spectrum Model

In static engine tests, the flow undergoes a large cross-stream contraction as it enters the inlet. This contraction produces highly anisotropic turbulence. For typical inlet geometries, the flow contraction is nearly axisymmetric. Thus it seems reasonable to assume that the turbulence is also axisymmetric. In this section, we will use the theory of axisymmetric turbulence[12] to develop a spectrum model that represents the highly anisotropic nature of inflow turbulence.

The statistical theory of axisymmetric turbulence is a generalization of isotropic theory in which the turbulence is allowed to have a preferred direction defined by the unit vector λ. Chandrasekhar[12] showed that the most general form for the velocity correlation tensor that satisfies the continuity equation and the appropriate symmetry requirements is

$$R_{ij}(\boldsymbol{x}) = \epsilon_{j\ell m}\frac{\partial q_{im}}{\partial x_\ell} \tag{7a}$$

$$q_{ij} = Q_1\epsilon_{ijk}x_k + \left[\lambda_j Q_2 + \frac{x_j}{x}\frac{\partial Q_1}{\partial \mu}\right]\epsilon_{i\ell m}\lambda_\ell x_m \tag{7b}$$

Here $\boldsymbol{x}$ represents the separation between the positions at which the velocities v_i and v_j are measured, and the coordinate system moves with the uniform mean flow. ϵ_{ijk} is the alternating tensor, $x=\sqrt{x_k x_k}$, $\lambda\cdot\boldsymbol{x}=\mu x$, and Q_1 and Q_2 are "arbitrary" functions of x and μx. A similar formulation for the energy spectrum tensor [the Fourier transform of $R_{ij}(\boldsymbol{x})$] can be derived. The result is

$$\Phi_{ij}(\boldsymbol{k}) = [k^2\delta_{ij} - k_i k_j]F + [(k^2 - (k_m\lambda_m)^2)\delta_{ij} - k_i k_j - k^2\lambda_i\lambda_j + k_m\lambda_m(\lambda_i k_j + k_i\lambda_j)]G \tag{8}$$

Here δ_{ij} is the substitution tensor and F and G are "arbitrary" functions of k and $(\boldsymbol{k}\cdot\lambda)$.

For our application we chose λ to be in the direction defined by the mean flow, i.e., the x_1 coordinate direction. Then we consider Q_1 and Q_2 as functions of x_1 and $\sigma=\sqrt{x_2^2+x_3^2}$ while F and G are functions of k_1 and $k_t=\sqrt{k_2^2+k_3^2}$. We must now choose particular expressions for Q_1 and Q_2 (or F and G) such that the proper turbulence intensities and length scales are obtained. The theory of Ref. 12 gives little guidance as to acceptable forms for these functions. While examining this question during an early phase of the present research, it was found that the functions Q_1 and Q_2 (or F and G) are not entirely arbitrary but must satisfy certain constraints. This is why the word "arbitrary" was placed in quotation marks in the preceding discussion. The constraints follow from a theorem[15,16] which assures that the power-spectral density of the turbulent velocity component in an arbitrary direction is non-negative for all values of the wavenumber. This condition is used in Ref. 17 to derive the following constraint equations for F and G.

$$F(k_1,k_t) \geq 0 \tag{9a}$$

$$k^2F(k_1,k_t) + k_t^2G(k_1,k_t) \geq 0 \tag{9b}$$

The equivalent constraints on Q_1 and Q_2 are given by

$$Q_1(x_1,\sigma) \geq Q_1(0,0) \tag{10a}$$

$$B(x_1,\sigma) \geq B(0,0) \tag{10b}$$

$$B = \frac{2}{\sigma}\frac{\partial}{\partial\sigma}(\sigma^2Q_1) + \frac{1}{\sigma}\frac{\partial}{\partial\sigma}(\sigma^2Q_2) - \frac{x_1^2}{\sigma}\frac{\partial}{\partial\sigma}\left(\sigma\frac{\partial Q_1}{\partial\sigma}\right) + 2\frac{x_1}{\sigma}\frac{\partial^2}{\partial x_1\partial\sigma}(\sigma^2Q_1) - \frac{\partial^2}{\partial x_1^2}(\sigma^2Q_1) \tag{10c}$$

Failure to satisfy these constraint equations can lead to very unrealistic results, such as negative values of the power-spectral density [Eqs. (3) and (5)] over a portion of the frequency spectrum.

Three different choices for the "arbitrary" functions were examined in detail. All these choices appeared to be reasonable in that the one-dimensional correlations were given by the commonly accepted forms

$$R_{11}(x_1) = u_a^2e^{-|x_1|/\ell_a} \qquad R_{22}(x_2) = u_t^2e^{-|x_2|/\ell_t}$$

where u_a, ℓ_a and u_t, ℓ_t are the turbulence rms velocities and integral length scales in the axial and tangential directions, respectively. However, it was found that only one of the three choices examined satisfied the preceding constraint equations.

The first choice examined was

$$Q_1 = -(u_a^2/2)e^{-y} \tag{11a}$$

$$Q_2 = (u_a^2 - u_t^2)e^{-y} \tag{11b}$$

where

$$y = [(x_1/\ell_a)^2 + (\sigma/\ell_t)^2]^{1/2}$$

This formulation was used in Ref. 18 to study the influence of turbulence anisotropy on jet noise. The constraint Eq. (10a) is satisfied for all choices of the turbulence intensities and length scales. To examine the constraints presented by Eq. (10b), we must calculate $B(x_1,\sigma)$. Since we are particularly interested in the large axial length scale case, we will examine the limit $(\ell_a/\ell_t) \gg 1$, while keeping the relative magnitudes of x_1, σ, u_a, and u_t arbitrary. Thus we obtain

$$B(x_1,\sigma) - B(0,0) = 2u_t^2[1-e^{-y}] + u_t^2\frac{e^{-y}}{y}\left(\frac{\sigma}{\ell_t}\right)^2 - \frac{u_a^2}{2}\frac{e^{-y}}{y}\left\{2\left(\frac{x_1}{\ell_t}\right)^2 + \left(\frac{\sigma}{\ell_a}\right)^2 - \left(\frac{x_1\sigma}{\ell_t^2}\right)^2\left(\frac{1}{y}+\frac{1}{y^2}\right)\right\}$$

In order to satisfy Eq. (10b), the right-hand side must be non-negative for all choices of x_1 and σ. It can be shown that the worst case occurs for $\sigma=0$. Examining this case, we see that the expression is non-negative for all values of x_1 only if $2(u_t/u_a)^2 \geq (\ell_a/\ell_t)^2$. The experimentally measured conditions do not satisfy this constraint, indicating that Eqs. (11) are not a suitable model for Q_1 and Q_2.

In order to evaluate the importance of satisfying the constraints, the spectrum model given by Eqs. (11) was incorporated into our noise prediction computer program. Calculations were made for a range of ℓ_a/ℓ_t, holding u_t/u_a fixed. As ℓ_a/ℓ_t was increased beyond the appropriate range defined by the constraint equations, the sound power decreased sharply and eventually became negative. Such a result is physically impossible, since sound power is a mean square quantity. Thus it appears that very serious errors can occur when turbulence models are used outside the range of validity defined by Eq. (9) or (10).

The second choice for Q_1 and Q_2 that was examined was

$$Q_1 = -\frac{u_a^2}{2}\exp\left[-\frac{|x_1|}{\ell_a} - \frac{\sigma}{\ell_t}\right] \tag{12a}$$

$$Q_2 = 2(u_t^2/u_a^2 - 1)Q_1 \tag{12b}$$

This formulation is similar to that used in Refs. 7 and 8. The first constraint Eq. (10a) is seen to be satisfied by Eq. (12a). However, when attempting to apply the second constraint Eq. (10b), it was found that the function $B(x_1,\sigma)$ is not defined at the origin. The behavior of $R_{22}(\boldsymbol{x})$ in the vicinity of the origin is also unacceptable. Thus the formulation given by Eqs. (12) is not a suitable model for the anisotropic turbulence.

The axisymmetric turbulence model used in the present study is given by

$$F=\frac{2\ell_a\ell_t^4u_a^2}{\pi^2z^3} \tag{13a}$$

$$G=\left[2\frac{u_t^2}{u_a^2}-\frac{\ell_t^2}{\ell_a^2}-1\right]F \tag{13b}$$

where

$$z=[1+\ell_a^2k_1^2+\ell_t^2k_t^2]^{1/2}$$

Application of Eqs. (9) shows that this model is valid for the case $2(u_t/u_a)^2\geq(\ell_t/\ell_a)^2$. The experimental conditions easily satisfy this constraint. The values of u_a, u_t, ℓ_t and ℓ_a are chosen independently in the present model, and thus the integral properties of the turbulence are characterized accurately. It would be useful to compare the shape of our three-dimensional spectrum model with experimental results. Unfortunately, only measurements of the one-dimensional spectra have been documented in any detail. Our spectrum model produces exponential decay for the one-dimensional correlations, and it is unlikely that any other simple shape would provide significantly better agreement with data. Until more detailed experimental results are available, it seems most reasonable to use a model that produces appropriate one-dimensional correlations and satisfies the fundamental statistical requirements. Of the turbulence models examined, only that given by Eqs. (13) satisfies the necessary statistical requirements.

To apply this spectrum model, we need to calculate the two-dimensional spectra

$$\tilde{\Phi}_{ij}(k_1,k_2)=\int_{-\infty}^{\infty}\Phi_{ij}(k_1,k_2,k_3)\,dk_3$$

Using Eqs. (8) and (13) we obtain

$$\tilde{\Phi}_{11}=\frac{u_a^2\ell_a\ell_t}{4\pi\tilde{z}^3}\left[1+3\frac{\ell_t^2k_2^2}{\tilde{z}^2}\right] \tag{14a}$$

$$\tilde{\Phi}_{12}=-\frac{3u_a^2\ell_a\ell_t^3k_1k_2}{4\pi\tilde{z}^5} \tag{14b}$$

$$\tilde{\Phi}_{22}=\frac{u_a^2\ell_a\ell_t}{4\pi\tilde{z}^3}\left[2\frac{u_t^2}{u_a^2}-\frac{\ell_t^2}{\ell_a^2}+3\frac{\ell_t^2k_1^2}{\tilde{z}^2}\right] \tag{14c}$$

where

$$\tilde{z}=[1+\ell_a^2k_1^2+\ell_t^2k_2^2]^{1/2}$$

IV. Large Axial Length Scale Limit

The calculation of the noise level at a given frequency generally involves an infinite summation as discussed in Sec. II. However, for the case of large axial length scale ($\ell_a/s\gg1$), the analysis simplifies considerably. The noise spectrum is then dominated by sharp peaks at the blade passing frequency and its harmonics, with negligible contributions elsewhere. The infinite summation, each term of which contains an integral, is simplified to a single integration that produces the total sound power in each spectrum peak. The characteristics of these sharp peaks will now be examined. The quantities of primary interest for a spectrum of this type are the total sound power contained in each peak and the width of the peak.

We will first show that, for large axial length scales, a particular term in the infinite summation in Eqs. (3) and (5) contributes to the sound power spectrum peak at only one harmonic of blade passing frequency. Equation (3b) indicates that the frequency dependence of the sound power is related to the behavior of the turbulence spectrum as a function of k_1. The spectrum functions, $\tilde{\Phi}_d$ and $\tilde{\Phi}_q$, are maximized at $k_1=0$ and their rate of drop off increases with (ℓ_a/s). Consider the frequency $f=Nf_b$, i.e., a multiple of blade passing frequency. For this frequency, the largest term in the infinite series in Eqs. (3) and (5) is $n=N$, for which $k_1=0$. The next largest terms ($n=N\pm1$) will have $k_1=\pm2\pi\tan\alpha/s$. For large enough values of ℓ_a/s, these terms will be insignificant. Thus in the limit of large axial length scale, the noise spectrum in the vicinity of $f=Nf_b$ is given by the single term, $n=N$ in Eqs. (3) and (5).

We now wish to find the total sound power associated with the peak at $f=Nf_b$. To do this, note that the functions $E_d^{\pm}$, $E_q^{\pm}$, and L do not vary rapidly in the vicinity of $k_1=0$, in contrast to $\tilde{\Phi}_d$ and $\tilde{\Phi}_q$. This can be shown formally by introducing normalized variables, $\kappa_1=\ell_ak_1$ and $\kappa_2=\ell_tk_2$. The turbulence spectra $\tilde{\Phi}_{ij}$ are then functions of κ_1 and κ_2 (independent of ℓ_a/s), while the other factors in Eqs. (3) and (5) are functions of the quantities $(\kappa_1s/\ell_a-2\pi N\tan\alpha)$ and $(\kappa_2s/\ell_t+2\pi N)$. We are interested in the case $(s/\ell_a)\ll1$, while $(s/\ell_t)=0(1)$. The functions $E_d^{\pm}$, L, $E_q^{\pm}$, and $\mathcal{G}_i$ can then be expanded in Taylor's series about $(s/\ell_a)=0$, i.e.,

$$E_d^{\pm}(\kappa_1,\kappa_2)=E_d^{\pm}(0,\kappa_2)+\kappa_1(s/\ell_a)E_{d_1}^{\pm}(\kappa_2)+\ldots$$

etc. Furthermore, the frequency (or k_1) dependence in the limits of integration over k_2 in Eqs. (3) and (5) is also $0(s/\ell_a)$. Thus, to lowest order in (s/ℓ_a), the frequency dependence of the sound power level in the vicinity of $f=Nf_b$ is only through $\tilde{\Phi}_{ij}$.

To determine the total sound power associated with the spectrum peak at $f=Nf_b$, we can integrate Eqs. (3) and (5) over frequency (or k_1). The dk_1 integral will be evaluated first. Thus setting

$$\hat{\Phi}_{ij}(k_2)=\int_{-\infty}^{\infty}\tilde{\Phi}_{ij}(k_1,k_2)\,dk_1$$

we obtain

$$\hat{\Phi}_{11}=\frac{u_a^2\ell_t}{2\pi\hat{z}^2}\left[1+2\frac{\ell_t^2k_2^2}{\hat{z}^2}\right] \tag{15a}$$

$$\hat{\Phi}_{22}=\frac{u_t^2\ell_t}{\pi\hat{z}^2} \tag{15b}$$

where

$$\hat{z}=[1+\ell_t^2k_2^2]^{1/2}$$

and $\hat{\Phi}_{12}$ is identically zero. The total dipole and quadrupole sound power levels associated with the peak at $f=Nf_b$ are then given by

$$P_{d_N}^{\pm}=\frac{U}{2\pi}\int\hat{\Phi}_d(k_2)E_d^{\pm}(0,k_2)L^2(\omega)\,dk_2 \tag{16a}$$

$$P_{q_N}^{\pm}=\frac{U}{2\pi}\int\hat{\Phi}_q(k_2)E_q^{\pm}(0,k_2)\,dk_2 \tag{16b}$$

where $\hat{\Phi}_d$ and $\hat{\Phi}_q$ are determined by replacing $\tilde{\Phi}_{ij}$ with $\hat{\Phi}_{ij}$ in Eqs. (4) and (6) and setting $k_1=0$ in the $\mathcal{G}_i$. We also set f/f_b and n equal to N in Eq. (3d) and $k_1=0$ in Eq. (3c). Note that the $\hat{\Phi}_{ij}(k_2)$ do not contain ℓ_a. Thus Eqs. (16) indicate that, for $(\ell_a/s)\gg1$, the total sound power is independent of (ℓ_a/s).

The maximum value of each spectrum peak occurs exactly at $f=fN_b$ $(k_1=0)$. This maximum value can be calculated from Eqs. (3) and (5). We see from Eqs. (14) that, for $(\ell_a/\ell_t)\gg1$, $\tilde{\Phi}_{ij}(0,k_2)$ is directly proportional to ℓ_a. Thus, in the large axial length scale limit, the maximum value of each spectrum peak increases linearly with (ℓ_a/s). The width of each spectrum peak must then be inversely proportional to

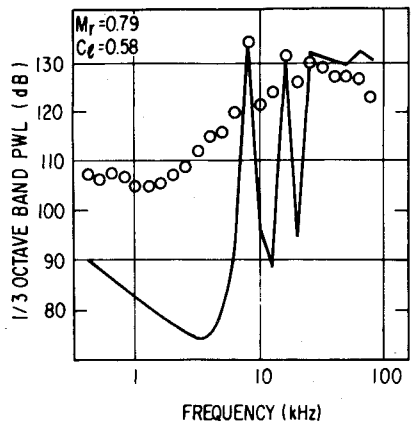

Fig. 2 Typical comparison of predicted and measured inlet PWL spectra for NASA rotor 11 without TCS: —— theory, o data.

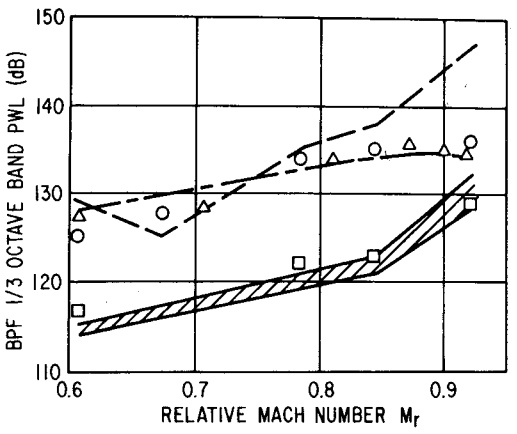

Fig. 3 Comparison of predicted and measured blade passing frequency inlet PWL as a function of relative Mach number; NASA rotor 11 without TCS: --- theory, o data; NASA rotor 11 with TCS: —— theory, □ data; QCSEE variable pitch fan —— theory, △ data.

Table 1 Turbulence properties in General Electric Corporate Research and Development anechoic chamber

	u_a/U_a	u_t/u_a	ℓ_a(m)	ℓ_a/ℓ_t
No TCS	0.015	2.0	2.9	300
With TCS	0.005	0.75	0.86	90-300

(ℓ_a/s), since for $(\ell_a/s) \gg 1$, the total sound power is independent of this parameter.

V. Comparison of Predictions with Experimental Data

The calculations presented in this section were made for two scale model fan stages[19,20] that were tested in the General Electric Corporate Research and Development anechoic chamber. These configurations were selected to evaluate the present rotor/turbulence interaction model because rather extensive sets of acoustic and turbulence data were available. The first fan stage, designated NASA rotor 11, was tested with and without an inlet turbulence control structure (TCS). The TCS[19,21] was designed to suppress incoming turbulence and thereby eliminate rotor/turbulence interaction noise. For the purposes of this study, however, the TCS produced different turbulence characteristics at the fan face and hence a second condition for theory/data comparison. Average values of the turbulence properties measured in Ref. 19 are listed in Table 1. For the case with TCS only the range of possible tangential length scales can be determined[22] due to measurement limitations. However, this will not significantly affect the theory/data comparison.

The NASA rotor 11 fan stage has a 0.508 m (20 in.) diam and is representative of typical high-speed aircraft engine fan designs. It has 44 blades and 86 vanes and a design tip speed of 425 m/s. Other details may be found in Ref. 19. Noise predictions were made using fan rotor geometric and aerodynamic conditions at the rms pitchline radius, defined as $r_p = \sqrt{(r_t^2 + r_h^2)}/2$. For NASA rotor 11, the blade spacing at the pitchline radius is $s = 2.9$ cm. Since the quadrupole component of the analysis has a singularity at $M_r = 1$, predictions were confined to subsonic relative Mach numbers.

The second fan stage[20] is a variable pitch design with 18 blades and 33 vanes, and a design tip speed of 306 m/s. Because of the variable pitch design this fan has a radially constant solidity, as opposed to conventional fixed blade fans that usually have radially constant chord and varying solidity. The data were taken without a TCS, and the pitchline rotor blade spacing is $s = 6.9$ cm. Other details can be found in Ref. 20.

A typical comparison of computed and measured one-third octave inlet quadrant PWL spectra for NASA rotor 11 without the TCS is shown in Fig. 2. It can be seen that the predictions of the blade passing frequency (BPF) tone and harmonics are in good agreement with the data, and that the predicted broadband levels are substantially below the measured level. The blade passing frequency for the case shown in Fig. 2 is approximately 6300 Hz and a BPF harmonic is present in every one-third octave band above 20,000 Hz. The predicted levels above 20,000 Hz are in good agreement with the measurements, but the predictions do not contain air attenuation effects. This would lower the prediction at the higher frequencies (by as much as 11 dB at 80 kHz). Examination of the measured narrowband spectrum shows that broadband rather than tone noise dominates the one-third octave bands above 30,000 Hz. The present prediction of random tone noise due to inflow turbulence would be consistent with this observation if air attenuation effects were accounted for.

For cases without the TCS, the comparisons of one-third octave spectra for NASA rotor 11 at other operating conditions and for the variable pitch fan were similar to that shown in Fig. 2. The comparisons for NASA rotor 11 with the TCS indicated that at open throttle conditions ($C_\ell = 0.58$) the rotor/turbulence interaction contributed only to the blade passing frequency tone, and that this noise source was insignificant at closed throttle conditions ($C_\ell = 0.78$). See Refs. 22 and 23 for details.

Figure 3 shows a comparison of measured and predicted blade passing frequency one-third octave levels as a function of relative Mach number. The agreement is reasonably good except at high speeds for rotor 11 without the TCS. The shaded band for rotor 11 with the TCS corresponds to the range of tangential length scales given in Table 1. The predicted noise level reduction with the TCS agrees well with the data. Comparisons were also made for the higher harmonics of blade passing frequency, but the results are less significant because rotor/stator interaction noise occurs at these frequencies. See Ref. 23 for details.

VI. Parametric Study

This section discusses the dependence of rotor/turbulence interaction noise on inlet turbulence properties. The calculations presented in this section were carried out for the NASA rotor 11 fan stage at 54% speed ($M_r = 0.61$, $C_\ell = 0.58$). Figure 4 shows the portion of the narrowband PWL spectrum centered around blade passing frequency, for a fixed transverse length scale of one blade spacing. We see that as axial length scale increases, the spectrum becomes more peaky. A doubling of axial length scale produces a 3 dB rise in the peak value of the spectrum, for $(\ell_a/s) \geq 50$. Thus, for large axial length scales, the peak values are proportional to (ℓ_a/s), in agreement with the analysis of Sec. IV.

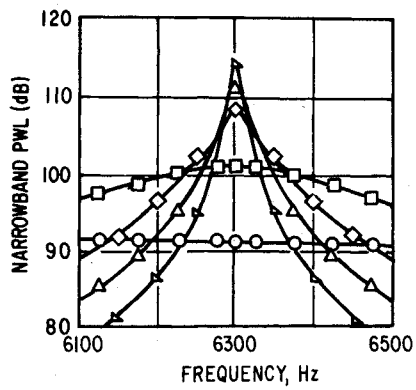

Fig. 4 Effect of axial length scale on predicted narrowband spectrum around blade passing frequency (6300 Hz) for NASA rotor 11 ($\ell_t/s=1$): ○ $\ell_a/s=1$, □ 10, ◇ 50, △ 100, ▲ 200.

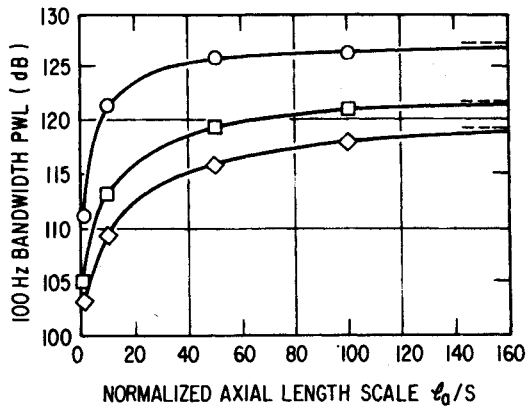

Fig. 5 Predicted effect of axial length scale on integrated 100 Hz bandwidth tone PWL: ○ BPF, □ 2×BPF, ◇3×BPF. Asymptotic values determined from large length scale approximation shown as dashed lines for comparison.

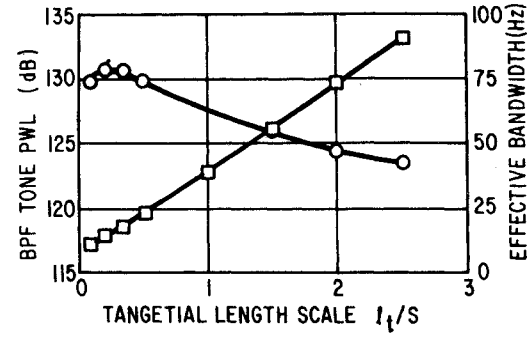

Fig. 6 Effect of tangential length scale on blade passing frequency tone for the large axial length scale approximation ($\ell_a/s=100$): ○ tone total PWL, □ tone width.

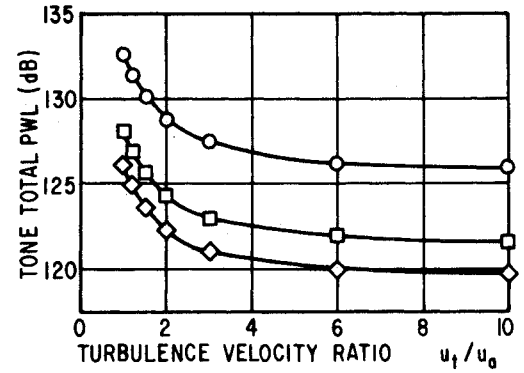

Fig. 7 Effect of turbulence velocity ratio on blade passing frequency and harmonic tone PWL for fixed transverse intensity ($u_t/U_a=0.03$): ○ BPF, □ 2×BPF, ◇ 3×BPF.

The large axial length scale approximation developed in Sec. IV implies that for $(\ell_a/s)\gg 1$ the total sound power should be independent of (ℓ_a/s). To examine this, the narrowband spectra were numerically integrated over 100 Hz bandwidths around blade passing frequency and its harmonics. The results for the first three harmonics are shown in Fig. 5. As expected, the total PWL in each 100 Hz bandwidth levels off with increasing (ℓ_a/s). The asymptotic values predicted from the large axial length scale limit are also shown as dashed lines in Fig. 5. It can be seen that for $(\ell_a/s)\geq 100$, the analysis of Sec. IV produces very accurate results. The spectra in Fig. 4 indicate that the differences at lower values of (ℓ_a/s) can be attributed partly to the narrow bandwidth used in the numerical integration. These differences would also decrease for smaller tangential length scales, see Fig. 6.

Figure 6 shows the variation in the spectrum peak at blade passing frequency as a function of tangential length scale, for the large axial length scale limit. The total sound power in the spectrum peak around blade passing frequency is maximized at $(\ell_t/s)=0.3$. The width of the spectrum peak is a monotonic function of (ℓ_t/s), with positive slope.

For turbulence properties typical of ground-based fan test facilities ($\ell_a/s=50$-100), it is interesting to compare the predictions of the present analysis with those of Hanson's model.[5] Both approaches produce strong narrowband peaks at the blade passing frequency harmonics, but Hanson's model also produces a substantial broadband noise level that is not predicted by the present analysis. Hanson's broadband noise level is associated with empirical constants that were chosen to produce agreement with pressure spectra measured by a blade mounted transducer. However, it is not clear that the broadband pressure fluctuations on the rotor blades are related directly to inflow turbulence. Perhaps they are caused by boundary-layer instabilities or transitory separation on the rotor blades. Experimental research would be necessary to clarify this issue.

The large inflow contraction that occurs in static fan test facilities amplifies the transverse component of turbulent velocity relative to the axial component. Typical rms velocity ratios are $(u_t/u_a)\approx 2$-4. The relative importance of the tangential and axial turbulence components on noise generation is illustrated as a function of (u_t/u_a) in Fig. 7. The sound power is reasonably constant for $(u_t/u_a)\geq 3$, indicating that in this region the noise is caused primarily by the transverse component of turbulence.

VII. Summary

An analytical model of fan noise generated by anisotropic inflow turbulence has been developed. The inflow turbulence representation is based on the statistical theory of axisymmetric turbulence. The predictions of the model were compared to experimental measurements in an anechoic chamber. The levels of the blade passing frequency and first few harmonics are in good agreement with the data, while the predicted broadband noise is far below the measured levels. For the large axial length scales typical of static fan test facilities, the total rotor/turbulence interaction sound power is practically independent of (ℓ_a/s). A simplified calculational procedure can be adopted in this situation. Because of the large inflow contraction that occurs in static fan tests, the transverse component of turbulent velocity is usually responsible for most of the rotor/turbulence interaction noise.

Acknowledgments

The work described herein was supported by the NASA Ames Research Center, Contract NAS2-10002, directed by Warren Ahtye.

References

[1] Gliebe, P. R., "Analytical Study of the Effects of Wind Tunnel Turbulence on Turbofan Rotor Noise," AIAA Paper 80-1022, 1980.

[2] Morfey, C. L., "Broadband Sound Radiated from Subsonic Rotors," *Proceedings of the International Symposium on Fluid Mechanics and Design of Turbomachinery*, Pennsylvania State Univ., 1970.

[3] Mani, R., "Noise Due to Interaction of Inlet Turbulence with Isolated Stators and Rotors," *Journal of Sound and Vibration*, Vol. 17, 1971, pp. 251-260.

[4] Homicz, C. F. and George, A. R., "Broadband Sound Radiation from Rotors in Turbulent Flow," *Interagency Symposium on University Research*, Stanford Univ., 1973.

[5] Hanson, D. B., "Spectrum of Rotor Noise Caused by Atmospheric Turbulence," *Journal of the Acoustic Society of America*, Vol. 56, July 1974, pp. 110-126.

[6] Pickett, G. F., "Effects of Nonuniform Inflow on Fan Noise," 87th Meeting of the Acoustical Society of America, 1974.

[7] Chandrashekara, N., "Tone Radiation from Axial Flow Fans Running in Turbulent Flow," *Journal of Sound and Vibration*, Vol. 18, 1971, pp. 533-543.

[8] Chandrashekara, N., "Sound Radiation from Inflow Turbulence in Axial Flow Fans," *Journal of Sound and Vibration*, Vol. 19, 1971, pp. 133-146.

[9] Mani, R., "Isolated Rotor Noise due to Inlet Distortion or Turbulence," NASA CR-2479, 1974.

[10] Mani, R. and Bekofske, K., "Experimental and Theoretical Studies of Subsonic Fan Noise," NASA CR-2660, 1976.

[11] Ribner, H. S. and Tucker, M., "Spectrum of Turbulence in a Contracting Stream," NACA Rept. 1113, 1951.

[12] Chandrashekhar, S., "The Theory of Axisymmetric Turbulence," *Philosophical Transactions of the Royal Society of London*, Series A, Vol. 242, 1950, pp. 557-577.

[13] Kemp, N. H., "Closed-Form Lift and Moment for Osborne's Unsteady Thin-Airfoil Theory," *AIAA Journal*, Vol. 11, Sept. 1973, pp. 1358-1360.

[14] Amiet, R. K., "High-Frequency Thin-Airfoil Theory for Subsonic Flow," *AIAA Journal*, Vol. 14, Aug. 1976, pp. 1076-1082.

[15] Cramer, H., "On the Theory of Stationary Random Processes," *Annals of Mathematics*, Vol. 41, 1940, pp. 215-230.

[16] Batchelor, G. K., *Theory of Homogeneous Turbulence*, Cambridge University Press, London, 1956, p. 25.

[17] Kerschen, E. J., "Constraint Equations for the Arbitrary Functions of Axisymmetric Turbulence," submitted to *Journal of Fluid Mechanics*.

[18] Goldstein, M. and Rosenbaum, B., "Effect of Anisotropic Turbulence on Aerodynamic Noise," *Journal of the Acoustical Society of America*, Vol. 54, 1973, pp. 630-645.

[19] Kantola, R. A. and Warren, R. E., "Reduction of Rotor-Turbulence Interaction Noise in Static Fan Noise Testing," AIAA Paper 79-0656, 1979.

[20] Bilwakesh, K. R., Clemons, A., and Stimpert, D. L., "Quiet Clean Short-Haul Experimental Engine (QCSEE) Acoustic Performance of a 50.8 cm Diameter Variable Pitch Fan and Inlet, Vol. I," NASA CR-135177, 1979.

[21] Ho, P. Y., Smith, E. B., and Kantola, R. A., "An Inflow Turbulence Reduction Structure for Scale Model Fan Testing," AIAA Paper 79-0655, 1979.

[22] Kerschen, E. J. and Gliebe, P. R., "Fan Noise Caused by the Ingestion of Anisotropic Turbulence—A Model Based on Axisymmetric Turbulence Theory," AIAA Paper 80-1021, 1980.

[23] Gliebe, P. R. and Kerschen, E. J., "Analytical Study of the Effects of Wind Tunnel Turbulence on Turbofan Rotor Noise," NASA CR 152359, 1979.